AADE-16-FTCE-84

Smart Foam Cement Characterization for Real Time Monitoring of Ultra-Deepwater Oil Well Cementing Applications

C. Vipulanandan and A. Reddy, Center for Innovative Grouting Materials and Technology (CIGMAT) and Texas Hurricane Center for Innovative Technology (THC-IT), University of Houston

Abstract

For a successful well cementing operation in deepwater under varying geological, temperature and pressure conditions in the boreholes, it is critical to monitor the flowing of the foam cement slurry between the casing and formation, depth of the circulation losses and fluid loss, setting of the foam cement in place and performance of the foam cement after hardening. The oil spill on the Gulf of Mexico in 2010 clearly demonstrated the need for the importance of monitoring foam cementing operations in real time from the time of placement through the entire service life of the well. At present there is no technology available to monitor cementing operations in real time from the time of placement through the borehole service life..

In this study, the behavior of smart oil well cement with varying amounts of foam was investigated. The oil well cement (Class H) with a water-to-cement (w/c) ration of 0.38 was modified with 0.1% conductive filler (CF) to make the cement very sensing and smart and the rheological properties, fluid loss and piezoresistivity (slurry and solid) behavior with 5% and 20% foam were investigated. The density of the smart cement was 16.3 ppg and with 20% foam it reduced to 9 ppg, a 45% reduction. Addition of 20% foam, reduced the thermal conductivity of the smart cement by 65%. Electrical resistivity was identified as the sensing and monitoring property for the smart foam cement. The smart cement slurries with and without foam were piezoresistive. With the addition of 20% foam, the resistivity change at 4 MPa (600 psi) increased from 8% for the smart cement slurry with no foam to 22% with 20% foam, about 175% increase in the piezoresistivity. The shear thinning behavior of the smart foam cement slurries have been quantified using the new hyperbolic rheological model and compared with another constitutive model with three material parameters, Herschel- Bulkley model. The results showed that the hyperbolic model predicated the shear thinning relationship for the smart foam cement slurries very well. The hyperbolic rheological model has a maximum shear stress limit were as the other model did not have a limit on the maximum shear stress. The maximum shear stress limit for smart cement slurry was 195 Pa and it reduced to 107 Pa with the addition of 20% foam, a 45% reduction. The total fluid loss for the smart cement at 0.7 MPa (100 psi) pressure was reduced from 134 mL to 13 mL with the addition of 20% foam, about a 90% reduction. The electrical resistivity changes of the hydrating cement was influenced by the amount of foam in the cement. Addition of 20% foam increased the initial electrical resistivity of smart cement from 1.05 Ωm to 2.04 Ωm, a 94% increase. The one day compressive strength of smart cement was reduced to 0.57 MPa (220 psi) from 10.3 MPa (1500 psi) with the addition of 20% foam, a 83% reduction. The solidified smart cement with and without foam were piezoresistive. The average percentage change in resistance at peak compressive stress of the smart foam cement with 20% foam after 1 day of curing was 113%, a 67% reduction compared to the smart cement without any foam. The average percentage change in resistance at peak compressive stress of the smart foam cement after 28 days of curing was 98%, about 490 times higher than the compressive strain at failure (0.2%) for smart cement without any foam. On an average the piezoresistivity after 28 days of curing was 18.6%/MPa, higher than the smart cement without any foam. A nonlinear piezoresistivity model has been developed to predict the piezoresistive behavior of the smart foam cement.

Introduction

Foam cement is a light weight and thermal insulating material consisting of cement matrix with porous structure created by injecting preformed foam into the cement slurry during the mixing process (Akthar et al. 2010). Foam cement is defined as a cementitious material having minimum of 20 percent by volume of foam in the slurry in which air pores are entrapped. But foam cement also present some disadvantages such as low ductility, low strength especially flexural strength (Li et al. 2008).

As deepwater exploration and production of oil and gas expands around the world, there are unique challenges in well construction beginning at the seafloor. Also preventing the loss of fluids to the formations and proper well cementing have become critical issues in well construction to ensure wellbore integrity because of varying downhole conditions (Labibzadeh et al. 2010; Eoff et al. 2009; Ravi et al. 2007; Gill et al. 2005; Fuller et al. 2002). Moreover the environmental friendliness of the cements is a critical issue that is becoming increasingly important (Durand et al. 1995; Thaemlitz et al. 1999; Dom et al. 2007). Lack of cement returns may

compromise the casing support and excess cement returns cause problems with flow and control lines (Ravi et al. 2007; Gill et al. 2005; Fuller et al. 2002). Hence there is a need for monitoring the cementing operation in real time. At present there is no technology available to monitor the cementing operation real time from the time of placement through the entire service life of the borehole. Also there is no reliable method to determine the length of the competent cement supporting the casing.

Two studies done on blowouts on the U.S. outer continental shelf during the period of 1971 to 1991 and 1992 to 2006 clearly identified cementing failures as the major cause for blowouts (Izon et al. 2007). Cementing failures increased significantly during the second period of study when 18 of the 39 blowouts were due to cementing problems (Izon et al. 2007). Also the deep-water horizon blowout in 2010 in the Gulf of Mexico was due to cementing issues (Carter et al. 2014; Kyle et al. 2014). The explosion at the drilling rig, Deepwater Horizon, which explored oil and gas at the Macondo well claimed eleven lives and caused severe injuries and record-breaking sea pollution by the release of about five million barrels of crude oil (Cristou and Konstantinidou 2012). Therefore, proper monitoring and tracking the process of well cementing and the performance during the entire service life has become important to ensure cement integrity (Vipulanandan et al. 2014 (a)-(d)).

Oil Well Cement

Oil well cementing is done to bond the casing to the formation so as to prevent blowout and to promote zonal isolation. The standards of API suggest the chemical requirements determined by ASTM procedures and physical requirements determined in accordance with procedures outlined in API RP 10B and ASTM. There are several types of cements that are being used for oil well cementing based on the oil well conditions. Oil-well cements (OWCs) are classified into grades based upon their $Ca_3Al_nO_p$ (Tricalcium Aluminate – C_3A) content. In general each class is applicable for a certain range of well depth, temperature, pressure, and sulphate environments. OWCs usually have lower C_3A contents and are coarsely ground with friction-reducing additives and special retarders such as starch and/or sugars in addition to or in place of gypsum.

Cements such as class G and class H, considered to be two of the popular cements, are used in oil well cementing applications. These cements are produced by pulverizing clinker consisting essentially of calcium silicates ($Ca_nSi_mO_p$) with the addition of calcium sulphate ($CaSO_4$) (John, 1992). When admixtures are added with cement, tensile and flexural properties will be modified. Also admixtures will have effect on the rheological, corrosion resistance, shrinkage, thermal conductivity, specific heat, electrical conductivity and absorbing (heat and energy) properties of oil well cement (Bao-guo, 2008). Oil well cement slurry is used several thousand feet below the ground level and hence determining cement setting time is always a challenge.

Light Weight Cements

Lightweight slurry of cement is said to slurries that their weight is 12 to 15 ppg (90 - 111 pcf). The lightest pure slurry that can be created is the slurry of cement of C Class. That if its w/c ratio sets to the desired number of 0.56, slurry with 15 ppg (111pcf) weight is achieved. If other classes of slurry are made with the w/c ratio that has been recommended by API, they will be heavier than this amount. Many of formation do not bear the hydrostatic pressure caused by these heavy slurries and for this reason they cannot be cemented with this kind of slurries. For cementing sections of an oil well which consist of weak and fragile zones, lighter slurry must be used. The easiest way to lighten slurry is adding the water to cement but the easiest way always is not the best way. Adding water to the cement slurry increases its w/c ratio and this leads to a reduction in slurry viscosity and subsequently deposition of suspended solids in the slurry. Aside from this disadvantage, water postpones thickening time of the slurry and dramatically reduces rock compression strength.

Cementing casing across highly depleted zones and weaker formations requires low-density cement systems capable of reducing the hydrostatic pressure of the fluid column during cement placement conditions.

Lightweight cement can be achieved in one of three ways:

- **Water extended**: Addition of more water (using high water to cement ratio). Slow compressive strength development and low ultimate compressive strength.
- **Foam cement:** Injecting gas (nitrogen, compressed air, or gas-generating solids) into the slurry provides the benefit of increased slurry compressibility, increase set-cement elasticity, and the flexibility to vary density during operations.
- **Microspheres:** Use of microspheres in combination with the conventional cements
  Solid, plastic beads of approximately 1.0 specific gravity;
  Hollow-pozzolanic spheres of approximately 0.7 specific gravity;
  Hollow glass bubbles of approximately 0.32 to 0.61 specific gravity.

Foam cements can help support both primary and remedial cementing functions for offshore and onshore situations, as indicated in the following list:

• Foam cements offer a low-density alternative to conventional cements. For example, slurries can be foamed to a density as low as 4 ppg. Low-density foamed cements (4 to 15 ppg) can be placed more easily across weak formations, helping prevent lost circulation and fallback problems;

• With some cement additives, foaming creates a synergistic effect that enhances the properties of the additives. This effect is evident with some fluid-loss additives, lost-circulation materials, and latex;

• The density of foamed cement is variable. Its ductility allows for expansion and pressure maintenance during

hydration, thus helping provide long-term zonal isolation. As the cement expands, it can fill washed-out hole sections and megadarcy lost-circulation zones without formation breakdown;

• The improved mud-removal capacity of foamed cement also helps enhance zonal isolation. Because of its ductility, foamed cement can provide casing support for the life of the well.

Foam cement

Foam cement provides particular benefits in to deepwater wells due to its lower thermal conductivity and enhanced flexibility. A low thermal conductivity cement sheath allows for less and slower heat transfer/heat loss in the wellbore. This benefit will allow for more productive steam-generating wells in geothermal projects. These enhanced mechanical properties will allow more flexibility for the cement sheath to respond to the effects of excessive temperatures in the wellbore, therefore maintaining cement sheath integrity and providing zonal isolation/casing protection. Enhanced and highly-engineered mechanical properties of the foam cement sheath allow it to move with the wellbore and also absorb stresses resulting from the mechanical shocks from pipe tripping to expansion and contraction of the casing during pressure and well testing, thermal shocks and during the injection and production cycling.

Importantly, foam cement is expected to establish a tight bond for a reliable annular seal because the nitrogen bubbles help to prevent shrinkage while the cement slurry goes through the hydration stage. A foamed system, due to its expansion properties, also accommodates challenging wellbore geometries such as wash-outs. It is important to note that foam cement has historically been used primarily for reduction of slurry density. Also foam cement systems much lighter than water, yet without compromising essential mechanical properties to establish life-of-the-well zonal isolation has been reported in the literature.

Piezoresistive Behavior

Banthia (1994) observed that strength and durability of concrete was improved by the addition of small amounts of fiber-reinforcement. Due to the fiber's high resistance to wear, heat, and corrosion, carbon fiber-reinforced concrete in particular has been shown to have excellent durability properties. Also, Chung (1996) reported that addition of carbon fiber to cement provided the strain-sensing ability and increased the tensile and flexural strengths, tensile ductility and flexural toughness, and decreased the drying shrinkage.

Chung (2001) studied the electrical resistivity of carbon fiber-reinforced cement paste and the electric polarization effect. By increasing the conductivity of the cement paste with carbon fibers that were more crystalline the polarization effect diminished. It was concluded that when the four-probe method was used, voltage polarity switching effects were dominated by the polarization of the sample itself, but when the two-probe method was used, voltage polarity switching effects were dominated by the polarization at the contact sample interface. Reza (2003) proved that with the addition of a small volume of carbon fibers into a concrete mixture produced a strong and durable concrete and made the product as a smart material. It is recommended that these techniques could be used as nondestructive testing methods to assess the integrity of the composite. Vipulanandan et al. (2004, 2005) studied the piezoresistive behavior of cementitious and polymer composites. The studies showed that the changes in resistivity with the applied stress were 30 to 50 times higher than the strain in the materials.

A smart cement has been developed (Vipulanandan et al. 2014a,b; Vipulanandan and Mohammed 2015a,b) which can sense any changes going on inside the borehole during cementing and during curing after cementing job. The smart cement can sense the water cement ratio, different additives, and any pressure applied to the cement sheath in terms of piezoresistivity (Vipulanandan and Mohammed 2015a). The failure compressive strain for the smart cement was 0.2% at peak compressive stress (Vipulanandan et al. 2015b) and the resistivity change is of the order of several hundreds make it more than 500 times more sensitive.

Theory and Concepts

It was very critical to identify the sensing properties for the cement and drilling mud that can be used to monitor the performance. After years of studies and based on the current study on oil well cements and drilling muds, electrical resistivity (ρ) was selected as the sensing property for cements (Vipulanandan et al. 2005, 2012). Hence two parameters (resistivity and change in resistivity) were used to quantify the sensing properties as follows:

$$R = \rho (L/A) = \rho K \quad \ldots\ldots (1)$$

Where

R = electrical resistance

L = Linear distance between the electrical resistance measuring points

A = effective cross sectional area

K = Calibration parameter is determined based on the resistance measurement method

Normalized change in resistivity with the changing conditions can be represented as follows:

$$\Delta\rho/\rho = \Delta R/R \quad \ldots\ldots (2)$$

The modified cement materials represented in terms of resistivity (ρ) to changes (composition, curing and stress) has been quantified to evaluate the sensitivity of the selected parameter.

Impedance Model (Vipulanandan et al., 2013)

Equivalent Circuit.

It is important to identify the most appropriate equivalent circuit to represent the electrical properties of a material to characterize its performace with time. There are many difficulties associated with choosing a correct equivalent circuit. It was necessary to somehow link the different elements in the circuit to different regions in the impedance data of the corresponding sample. Given the difficulties and uncertainties in establishing this link, researchers tend to take a pragmatic approach and adopt a circuit which they believe to be most appropriate from their knowledge of the expected behavior of the material under study, and demonstrate that the results are consistant with the circuit used.

In this study, different possible equivalent circuits were analyzed to find an appropriate equivalent circuit to represent smart cement and drilling mud.

Case 1: General Bulk Material –Capacitance and Resistance

In the equivalent circuit for Case1, the contacts were connected in series, and both the contacts and the bulk material were represented using a capacitor and a resistor connected in parallel (Fig. 1).

In the equivalent circuit for Case 1, R_b and C_b are resistance and capacitance of the bulk material, respectively; and R_c and C_c are resistance and capacitance of the contacts, respectively. Both contacts are represented with the same resistance (R_c) and capacitance (C_c), as they are identical. Total impedance of the equivalent circuit for Case 1 (Z_1) can be represented as follows:

$$Z_1(\sigma) = \frac{R_b(\sigma)}{1+\omega^2 R_b^2 C_b^2} + \frac{2R_c(\sigma)}{1+\omega^2 R_c^2 C_c^2} - j\left\{\frac{2\omega R_c^2 C_c(\sigma)}{1+\omega^2 R_c^2 C_c^2} + \frac{\omega R_b^2 C_b(\sigma)}{1+\omega^2 R_b^2 C_b^2}\right\}, \quad (3)$$

where ω is the angular frequency of the applied signal. When the frequency of the applied signal is very low, $\omega \rightarrow 0$, $Z_1 = R_b + 2R_c$, and when it is very high, $\omega \rightarrow \infty$, $Z_1 = 0$.

Case 2: Special Bulk Material - Resistance Only

Case 2 is a special case of Case 1 in which the capacitance of the bulk material (C_b) is assumed to be negligible (Fig. 2). The total impedance of the equivalent circuit for Case 2 (Z_2) is as follows:

$$Z_2(\sigma) = R_b(\sigma) + \frac{2R_c(\sigma)}{1+\omega^2 R_c^2 C_c^2} - j\frac{2\omega R_c^2 C_c(\sigma)}{1+\omega^2 R_c^2 C_c^2}. \quad (4)$$

When the frequency of the applied signal is very low, $\omega \rightarrow 0$, $Z_2 = R_b + 2R_c$, and when it is very high, $\omega \rightarrow \infty$, $Z_2 = R_b$ (Fig. 3).

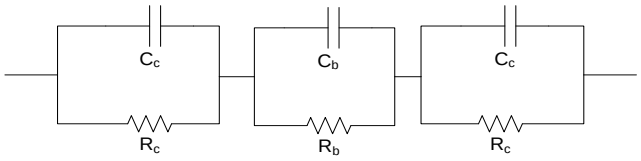

Figure 1. Equivalent Circuit for Case1

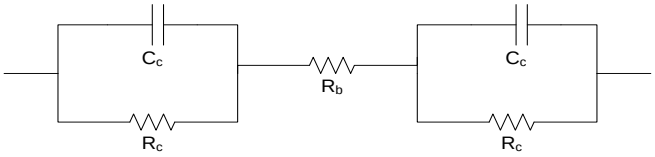

Figure 2. Equivalent Circuit for Case 2

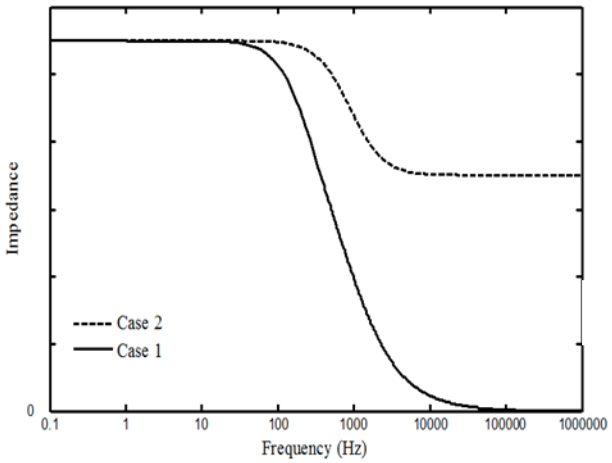

Figure 3. Comparison of Typical Responses of Equivalent Circuits for Case 1 and Case 2

The shape of the curves shown in Fig. 3 is very much influenced by material response and the two probe instruments used for monitoring. Testing of smart cement indicated that Case 2 represented there behavior and hence the bulk material properties can be represented by resistivity and characterized at a frequency of 300 kHz using the two probes.

Rheological Modeling

The cement slurry showed non-linear shear thinning behavior with a yield stress. Based on the test results, following conditions have to be satisfied for the model to represent the observed behavior.

Hence the conditions are as follows:

$$\tau = \tau_o \text{ when } \dot{\gamma} = 0$$

$$\frac{d\tau}{d\dot{\gamma}} > 0 \quad (5)$$

$$\frac{d^2\tau}{d\dot{\gamma}^2} < 0 \quad (6)$$

$$\dot{\gamma} \to \infty \Rightarrow \tau = \tau^* \quad (7)$$

The rheological models used for predicating the shear thinning behavior of foam cement slurry are as follows:

Herschel-Bulkley model (1926)

The Bingham plastic model includes both yield stress (τ_o) and a limiting viscosity (μ) at finite shear rates, which the Power law model fails to consider. For a nonlinear flow relationship shear-thinning or shear thickening behavior may be observed and the assumption of constant plastic viscosity is not valid. The Herschel-Bulkley (Eqn. 8) model defines a fluid with three parameters and can be represented mathematically as follows:

$$\tau = \tau_{o1} + k * (\dot{\gamma})^n \quad (8)$$

where τ , τ_{o1}, $\dot{\gamma}$, k and n represent the shear stress, yield stress, shear strain rate, correction parameter and flow behavior index respectively. For $\tau < \tau_o$ the material remains rigid. The model assumes that below the yield stress (τ_o), the slurry behaves as a rigid solid, similar to the Bingham plastic model. For $\tau > \tau_o$ the material flows as a Power law fluid. The exponent n describes the shear thinning and shear thickening behavior. Slurries are considered as shear thinning when n <1 and shear thickening when n >1. A fluid becomes shear thinning when the apparent viscosity decreases with the increase in shear strain rate.

Hence the model should satisfy the following conditions (Eqns. (5), (6) and (7)).

$$\frac{d\tau}{d\dot{\gamma}} = k*n*\dot{\gamma}^{(n-1)} > 0 \Rightarrow k*n > 0 \quad (9)$$

$$\frac{d^2\tau}{d\dot{\gamma}^2} = k * n(n-1) * \dot{\gamma}^{(n-2)} \Rightarrow \mathrm{k} * \mathrm{n} * (\mathrm{n}-1) < 0 \quad (10)$$

One condition when both Eqn (7) and Eqn. (8) will be satisfied is as follows:

$0 < n < 1$ and $k_1 > 0$.

From the Eqn. (8)

When $\dot{\gamma} \to \infty \Rightarrow \tau_{max.} = \infty$

Hence Herschel-Bulkley model doesn't satisfy the upper limit condition for the shear stress limit.

Hyperbolic model (2014)

Hyperbolic relationship between shear stress and shear strain rate for the oil well cement slurry with different temperature was investigated (Vipulanandan and Mohammed 2014).

$$\tau - \tau_{o2} = \frac{\dot{\gamma}}{C + D*\dot{\gamma}} \quad (11)$$

where τ: shear stress (Pa); τ_{o2}: yield stress (Pa); C (Pa. s)$^{-1}$ and D (Pa)$^{-1}$: are model parameters (Table 1) and $\dot{\gamma}$: shear strain rate (s^{-1}).

$$\frac{d\tau}{d\dot{\gamma}} = \frac{(C + D\dot{\gamma}) - \dot{\gamma} * D}{(C + D\dot{\gamma})^2} = \frac{C}{(C + D\dot{\gamma})^2} > 0 \Rightarrow C > 0$$

$$\frac{d^2\tau}{d\dot{\gamma}^2} = \frac{-2CD}{(C + D\dot{\gamma})^3} < 0 \Rightarrow D > 0$$

Also when $\dot{\gamma} \to \infty \Rightarrow \tau_{\max} = \frac{1}{D} + \tau_{o2}$ (12)

Hence this model has a limit on the maximum shear stress; the slurry will produce at relatively high rate of shear strains.

Objectives

The overall objective was to quantify the effect of foam content on the electrical resistivity, rheological properties, fluid loss and piezoresistive behavior of smart oil well cement. The specific objectives are as follows:

(i) Characterize the rheological properties (shear stress - shear strain rate relationship) of smart foam cement at different foam contents and model the behavior using hyperbolic model and Herschel-Bulkley model.

(ii) Investigate the piezoresistivity and fluid loss characteristics of the smart foam cement slurry.

(iii) Characterize the curing of the solidified foam cement and quantify the piezoresistive behavior of smart foam cement with different foam contents up to 28 days of curing.

Materials and Methods

Foam cement

In this study, Class H cement with water-to-cement of 0.38 was used. The samples were prepared according to the API standards. To improve the sensing properties and piezoresistive behavior of the cement modified with 0.1% of conductive fillers (CF) by the weight of the cement was mixed with all the samples. Commercially available foam was added to the cement slurry and mixed for at least for 5 minutes. After mixing, cement slurries with and without foam were used for rheological, fluid loss, curing and piezoresistivity studies. For the curing and compressive behavior studies cement slurry was cast in plastic cylindrical molds with diameter of 50 mm and a height of 100 mm. Two conductive wires were placed in all of the molds to measure the changing in electrical resistivity. At least three specimens were tested under each condition investigated in this study.

Initial resistivity of smart cement slurry

Two Different methods were used for electrical resistivity measurements of oil well cement slurries. To assure the repeatability of the measurements, the initial resistivity was measured at least three times for each cement slurry type and the average resistivity was reported. The electrical resistivity of the cement slurries were measured using the conductive probe and digital resistivity meter.

Conductivity probe

Commercially available conductivity probe was used to measure the conductivity (inverse of resistivity) of the slurries. In the case of cement, this meter was used during the initial curing of the cement. The conductivity measuring range was from 0.1μS/cm to 1000 mS/cm, representing a resistivity of 0.1Ω.m to 10,000 Ω.m.

Digital resistivity meter

Digital resistivity meter (used in the oil industry) was used measure the resistivity of fluids, slurries and semi-solids directly. The resistivity range for this device was 0.01 Ω -m to 400 Ω -m.

The conductivity probe and the digital electrical resistivity device were calibrated using standard solution of sodium chloride (NaCl).

Thermal Conductivity

The thermal conductivity of the cement slurries were measure using a commercially available thermal conductivity probe.

Resistivity of smart cement

In this study high frequency AC measurement was adopted to overcome the interfacial problems and minimize the contact resistances. Electrical resistance (R) was measured using LCR meter during the curing time. This device has a least count of 1 μΩ for electrical resistance and measures the impendence (resistance, capacitance and inductance) in the frequency range of 20 Hz to 300 kHz. Based on the impedance (z) – frequency (f) response it was determined that the smart cement was a resistive material (Vipulanandan et al. 2013). Hence the resistance measured at 300 kHz using the two probe method was correlated to the resistivity (measured using the digital resistivity device) to determine the K factor (Eqn.1) for a time period of initial five hours of curing. This K factor was used to determine the resistivity of the cement with the curing time.

Piezoresistivity test

Piezoresistivity describes the change in electrical resistivity of a material under stress. In this study both cement slurry and solidified cement will be tested and characterized. Since oil well cement serves as pressure-bearing part of the oil and gas wells in real applications, the piezoresistivity of smart cement (stress – resistivity relationship) with different w/c ratios were investigated under compressive loading at different curing times. During the compression test, electrical resistance was measured in the direction of the applied stress. To eliminate the polarization effect, AC resistance measurements were made using a LCR meter at frequency of 300 kHz (Vipulanandan et al. 2013).

Rheological test

The rheology tests for smart cement with different water-to-cement ratios at two different temperature of 25°C and 85°C were tested using a viscometer in the speed range of 0.3 to 600 rpm (shear strain rate of 0.5 s^{-1} to 1024 s^{-1}) with a heating chamber. The speed accuracy of this device was 0.001 rpm. The temperature of the slurry was controlled to an accuracy of ±2˚C. The viscometer was calibrated using several standard solutions. All the rheological tests were performed after 10 minutes of mixing of the cement slurries.

Compressive strength test

The cylindrical specimens (50 mm dia.*100 mm height) were capped and tested at a predetermined controlled displacement rate. Compression tests were performed on cement samples after 1 day and 28 days of curing using a hydraulic compression machine.

Results and Discussion

Cement Slurry

Density

The density of the cement slurry with a water-to-

cement ratio of 0.38 was 16.3 ppg. Addition of 5% foam (based on total weight of the cement slurry) reduced the density to 12.8 ppg, 21.5% reduction. Increasing the foam content to 20%, reduced the density to 9 ppg, a 45% reduction.

Thermal Conductivity

The thermal conductivity of the cement slurry with a water-to-cement ratio of 0.38 was 0.802 W/mK. Addition of 5% foam (based on total weight of the cement slurry) reduced the thermal conductivity to 0.482 W/mK, 40% reduction. Increasing the foam content to 20%, reduced the thermal conductivity to 0.284 W/mK, a 65% reduction.

Piezoresistivity

The cement slurries with and without foam were subjected to pressure up to 4 MPa in the high pressure high temperature chamber (HPHT) to investigate the piezoresistive behavior.

0% Foam: The resistivity of the smart cement slurry decreased nonlinearly with increase in the pressure (Fig. 4). At 4 MPa pressure the decrease in resistivity was 8%, indicating the piezoresistivity characteristics of the smart cement slurry.

5% Foam: The resistivity of the smart cement slurry with 5% foam decreased nonlinearly with increase in the pressure (Fig. 4). At 4 MPa pressure the decrease in resistivity was 12%, indicating the piezoresistivity characteristics of the smart cement slurry. With 5% foam the piezoresistivity characteristics of the smart foam cement slurry increased by 50%.

20% Foam: The resistivity of the smart cement slurry with 20% foam decreased nonlinearly with increase in the pressure (Fig. 4). At 4 MPa pressure the decrease in resistivity was 22%, indicating the piezoresistivity characteristics of the smart cement slurry. With 20% foam the piezoresistivity characteristics of the smart foam cement slurry increased by 175%, making the smart foam cement to be more sensing.

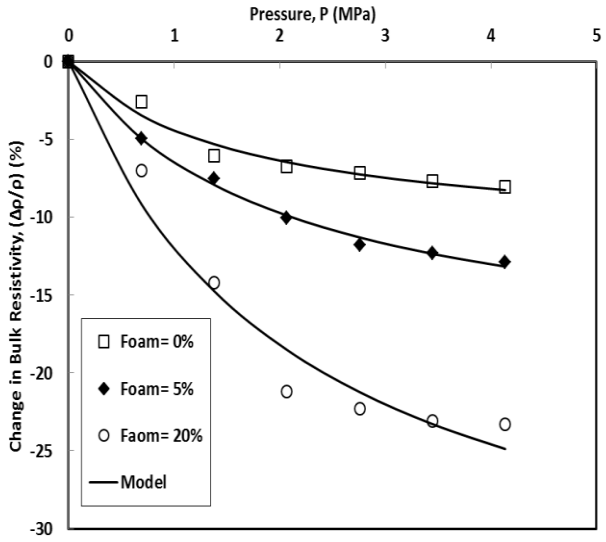

Figure 4 Measured and Predicted Stress-Resistivity Relationship for the Smart Cement With and Without Foam

Rheological Properties

Shear stress – shear strain rate relationships for smart foam cement were predicated using the hyperbolic model and compared with Herschel- Bulkley model as shown in Fig. 3. Also all the model parameters are summarized in Table 1 with root mean square error (RMSE) and coefficient of determination for all the predictions.

Herschel-Bulkley model (1926)

0% Foam: The shear thinning behavior of smart cement slurry with w/c ratio of 0.38 at a temperature of 25°C was tested and modeled using the Herschel-Bulkley model (Eqn. (6)) up to a shear strain rate of 1024 s^{-1} (600 rpm). The coefficient of determination (R^2) was 0.98 as summarized in Table 1. The root mean square of error (RMSE) was 5.38 Pa. The average yield stress (τ_{o1}) for the cement slurry at temperature of 25°C was 29 Pa. The model parameter k for the cement slurry with w/c ratio of 0.38 at 25°C was 16.7 Pa.s^n as summarized in Table 1. The model parameter n for the cement slurry was 0.31.

5% Foam: The shear thinning behavior of smart cement slurry with 5% foam at a temperature of 25°C was tested and modeled using the Herschel-Bulkley model (Eqn. (6)) up to a shear strain rate of 1024 s^{-1} (600 rpm). The coefficient of determination (R^2) was 0.98 as summarized in Table 1. The root mean square of error (RMSE) was 5.29 Pa. The average yield stress (τ_{o1}) for the cement slurry at temperature of 25°C was 13 Pa, a reduction of 55% compared to the smart cement without any foam. The model parameter k for the 5% foam

cement slurry was 8.7 Pa.s^n a reduction of 11% compared to the smart cement without any foam. The model parameter n for the 5% foam cement slurry was 0.36.

20% Foam: The shear thinning behavior of smart cement slurry with 20% foam at a temperature of 25^{o}C was tested and modeled using the Herschel-Bulkley model (Eqn. (6)) up to a shear strain rate of 1024 s^{-1} (600 rpm). The coefficient of determination (R^2) was 0.99 as summarized in Table 1. The root mean square of error (RMSE) was 1.58 Pa. The average yield stress (τ_{o1}) for the cement slurry at temperature of 25^{o}C was 5 Pa, a reduction of 83% compared to the smart cement without any foam. The model parameter k for the 20% foam cement slurry was 1.2 Pa.s^n a reduction of 93% compared to the smart cement without any foam. The model parameter n for the foam cement slurry was 0.55, an increase of 77% compared to the smart cement without any foam..

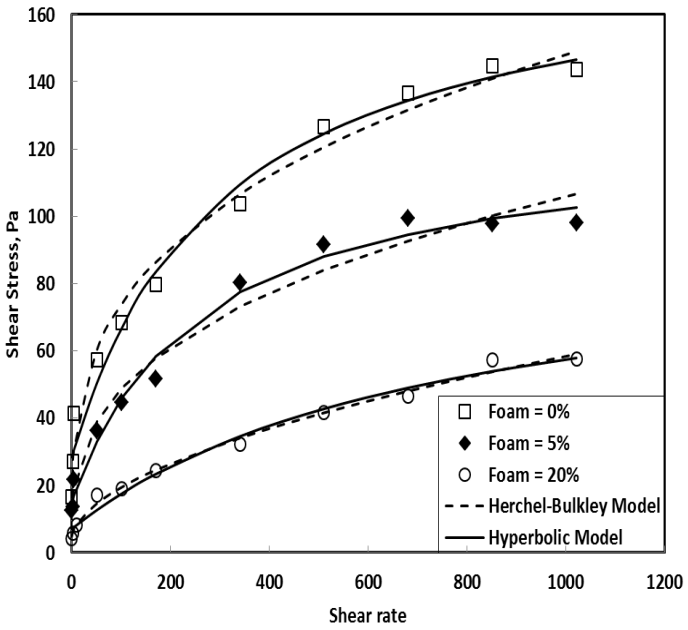

Figure 5 Measured and Predicted Shear Stress-Shear Strain Rate Relationship for the Smart Cement With and Without Foam

Hyperbolic model (Vipulanandan et al. 2014)

0% Foam: The shear thinning behavior of smart cement slurry with w/c ratio of 0.38 at a temperature of 25^{o}C was tested and modeled using the Hyperbolic model (Eqn. (9)) up to a shear strain rate of 1024 s^{-1} (600 rpm). The coefficient of determination (R^2) was 0.98 as summarized in Table 1. The root mean square of error (RMSE) was 5.68 Pa. The average yield stress (τ_{o1}) for the cement slurry at temperature of 25^{o}C was 28 Pa. The model parameter C for the cement slurry with w/c ratio of 0.38 at 25^{o}C was 1.97 Pa.s^{-1} as summarized in Table 1. The model parameter D for the cement slurry was 0.006 Pa^{-1}.

5% Foam: The shear thinning behavior of smart cement slurry with 5% foam at a temperature of 25^{o}C was tested and modeled using the Hyperbolic model (Eqn. (9)) up to a shear strain rate of 1024 s^{-1} (600 rpm). The coefficient of determination (R^2) was 0.99 as summarized in Table 1. The root mean square of error (RMSE) was 3.82 Pa. The average yield stress (τ_{o1}) for the cement slurry at temperature of 25^{o}C was 15 Pa, a reduction of 46% compared to the smart cement without any foam. The model parameter C for the 5% foam cement slurry was 2.34 Pa.s^{-1} an increase of 19% compared to the smart cement without any foam. The model parameter D for the 5% foam cement slurry was 0.009.

20% Foam: The shear thinning behavior of smart cement slurry with 20% foam at a temperature of 25^{o}C was tested and modeled using the Hyperbolic model (Eqn. (9)) up to a shear strain rate of 1024 s^{-1} (600 rpm). The coefficient of determination (R^2) was 0.99 as summarized in Table 1. The root mean square of error (RMSE) was 2.3 Pa. The average yield stress (τ_{o1}) for the cement slurry at temperature of 25^{o}C was 7 Pa, a reduction of 75% compared to the smart cement without any foam. The model parameter C for the 20% foam cement slurry was 8.49 Pa.s^{-1} an increase of 331% compared to the smart cement without any foam. The model parameter D for the foam cement slurry was 0.01.

Table.1. Herchel-Bulkley and hyperbolic rheological model parameters for smart cement slurries with foam

Foam Content (%)	Herchel-Bulkley Model (1926)					Hyperbolic Model (2014)					
	τ_{o1}(Pa)	K (Pa s^n)	n	RMSE (Pa)	R^2	τ_{o2} (Pa)	C (Pa s^{-1})	D (pa)$^{-1}$	τ_{max} (Pa)	RMSE (Pa)	R^2
0	29 ± 1.7	16 ± 0.03	0.31 ± 0.01	5.38	0.98	28 ± 2.5	1.97 ± 0.1	0.006 ± 0.001	195 ± 3.6	5.68	0.98
5	13 ± 1.2	8.7 ± 0.05	0.36 ± 0.01	5.29	0.98	15 ± 1.3	2.34 ± 0.1	0.009 ± 0.001	126 ± 2.1	3.82	0.99
20	5 ± 0.95	1.2 ± 0.06	0.55 ± 0.02	1.58	0.99	7 ± 1.1	8.49 ± 0.15	0.01 ± 0.002	107 ± 1.6	2.3	0.99

Maximum shear stress ($\tau_{max.}$)

Based on Eqn. (12) the hyperbolic model has a limit on the maximum shear stress ($\tau_{max.}$) the slurry will produce at relatively very high rate of shear strains. The τ_{max} for smart cement slurries with 0%, 5% and 20% foam at temperature of 25°C were 195 Pa, 126 Pa and 107 Pa respectively as summarized in Table 1. Hence, with 20% foam the maximum shear stress was reduced by 45%.

Fluid Loss

The total fluid loss from the cement slurry at pressure of 0.7 MPa (100 psi) with a water-to-cement ratio of 0.38 was 134 mL (Fig. 6). Addition of 5% foam (based on total weight of the cement slurry) reduced the fluid loss to 31.4 mL, 77% reduction. Increasing the foam content to 20%, reduced the fluid loss to 13.7 mL, a 90% reduction. A hyperbolic model was used to predict the fluid loss with time (Vipulanandan 2014)

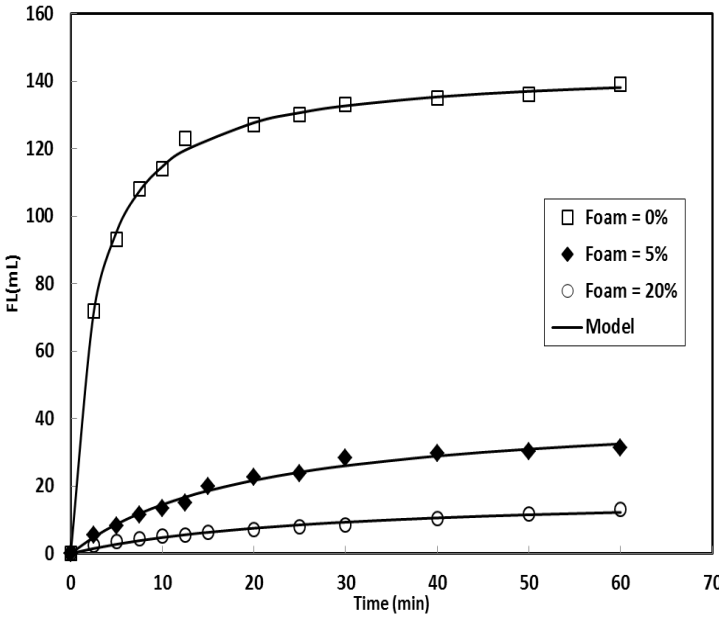

Figure 6 Measured and Predicted Fluid Loss- Time Relationship for the Smart Cement with and Without Foam

Curing of smart cement

Impedance Vs Frequency Curves

Investigation of the impedance versus frequency relationship tested after 1 day and 28 days of curing for smart foam cement with 20% foam is shown in Fig. &. The observed shape of the curve represents the Case 2 in Fig. 3, indicating that the bulk material can be represented by resistance.

.

Resistivity of the curing cement sheath with time

The resistivity of the cement slurry with curing time of up to 28 days was determined from the samples in small molds (2 inches diameter and 4 inches height cylindrical mold) cured under room condition. The normal trend of the resistivity of the cured cement is that the resistivity decreased up to a certain time (t_{min}) and reached to a minimum resistivity (ρ_{min}) and then starts increase with time. The initial resistivity of the cement with 0%, 5% and 20% form were 1.05 Ωm, 1.2 Ωm and 2.04 Ωm. Hence the addition of 20% foam increased the initial resistivity of the smart foam cement by 94%. Also the maximum percentage resistivity change was represented by RI_{24} ($(\rho_{24}-\rho_{min})/\rho_{min}$x100%) The RI24 for smart foam cement with 0%, 5% and 20% foam content were 230%, 133% and 6% respectively (Table 2).

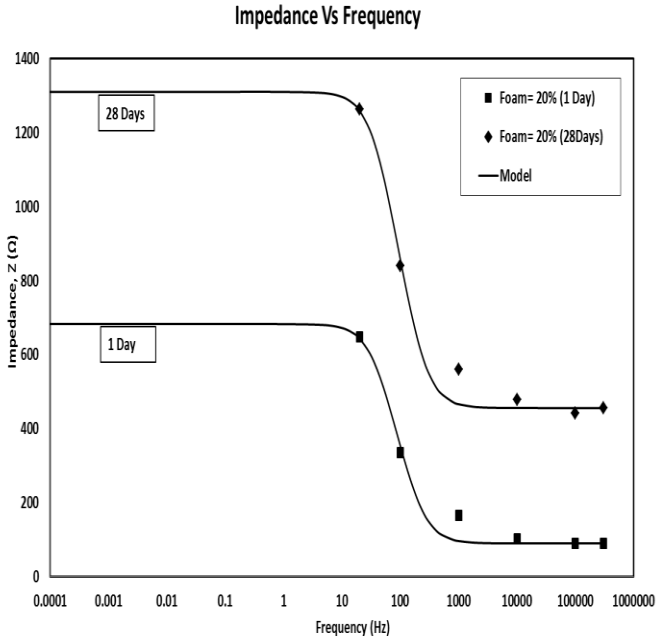

Figure 7 Measured and Predicted Fluid Loss- Time Relationship for the Smart Cement With and Without Foam

At least three specimens were tested and the average results about the variation in the resistivity with time up to 1 day and 28 days of curing are presented in Fig. 8. Hence the nonlinear model proposed by Vipulanandan and Paul (1990) was modified and used to predict the changes in the electrical resistivity of cement during hydration under different curing conditions and curing time. The proposed curing model is as follows:

$$\frac{1}{\rho} = \left(\frac{1}{\rho_{min}}\right)\left[\frac{\left(\frac{t+t_o}{t_{min}+t_o}\right)}{q_1+(1-p_1-q_1)*\left(\frac{t+t_o}{t_{min}+t_o}\right)+p_1*\left(\frac{t+t_o}{t_{min}+t_o}\right)^{\frac{q_1+p_1}{p_1}}}\right] \quad (13)$$

Where, ρ is the electrical resistivity (Ω-m); ρ_{min} is the minimum electrical resistivity (Ω-m); t_{min} is the time to reach the minimum electrical resistivity (ρ_{min}). The model parameters were t_o, p_1 (t) and q_1 (t) and t was the curing time (min). The parameter q_1 represents the initial rate of change in the resistivity.

There are three characteristic resistivity parameters that can be used in monitoring the curing (hardening process) of the cement. The resistivity parameters are the initial resistivity (ρ_o), minimum electrical resistivity (ρ_{min}) and time to reach the minimum resistivity (t_{min}).

The resistivity shows an increasing trend with curing time (Fig. 8) which has been modeled with the curing model which is developed by modifying the p-q model proposed by Vipulanandan and Paul (1990) (Eqn. 13). The model parameters were for moisture control curing (zero weight loss): p_1=0.65, q_1=0.281, and t_o=80 min; for room curing: p_1=0.41, q_1=0.151, and t_o=50 min; and for under water curing: p_1=0.19, q_1=0.082, and t_o=45 min. (Table 2).

The resistivity of smart cement with zero foam after 28 days of curing was 14.5 Ωm, hence the percentage change in resistivity was 1283%. The resistivity of the 20% foam cement after 28 days of curing was 12.5 Ωm, percentage change in resistivity in 28 days was 520%.

Compressive Behavior

Strength

0% Foam: The average compressive strength of the smart cement after 1 day of curing was 10.3 MPa. The average compressive strength of the smart cement after 28 days of curing was 19.7 MPa, a 91% increase in strength.

5% Foam: The average compressive strength of the smart foam cement after 1 day of curing was 4.6 MPa, about 55% reduction in strength compared smart cement without any foam. The average compressive strength of the smart foam cement after 28 days of curing was 14.6 MPa, a 217% increase in strength. The 28th day compressive strength of smart foam cement was 26% less than compressive strength of the smart cement without any foam.

20% Foam: The average compressive strength of the smart foam cement after 1 day of curing was 0.57 MPa, about 94% reduction in strength compared smart cement without any foam. The average compressive strength of the smart foam cement after 28 days of curing was 5.27 MPa, a 825% increase in strength. The 28th day compressive strength of smart foam cement was 73% less than compressive strength of the smart cement without any foam.

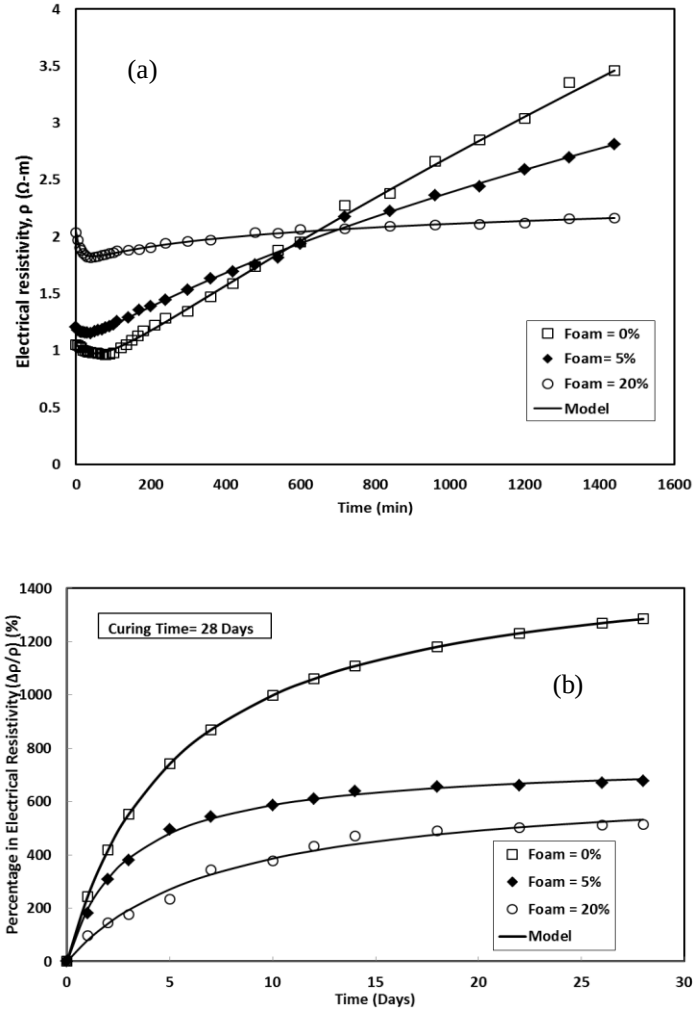

Figure 8 Measured and Predicted Resistivity- Time Relationship for the Smart Cement with and Without Foam

Table .2. Summary of bulk resistivity parameters for cement with various foam contents

Foam Content (%)	Initial Resistivity, ρ_o (Ω-m)	ρ_{min} (Ω-m)	t_{min} (min)	$\rho_{24\,h}$ (Ω-m)	RI_{24} (%)	p	q	t_0 (min)
0	1.05 ± 0.03	0.96 ± 0.01	98 ± 5.0	3.46 ± 0.02	230	0.65	0.281	80
5	1.2 ± 0.02	1.15 ± 0.03	55 ± 4.5	2.8 ± 0.02	133	0.41	0.151	50
20	2.04 ± 0.04	1.81 ± 0.04	43 ± 3.5	2.16 ± 0.02	6	0.19	0.082	15

Piezoresistiviy

Additional of 0.1% CF substantially improved piezoresistive behavior of the cement. Based on the experimental results, p-q model (Eqn. 14) was modified and used to predict the change in electrical resistivity of cement during with applied stress for 1 day and 28 days of curing. The model is defined as follows:

$$\frac{\sigma}{\sigma_f} = \left[\frac{\frac{x}{x_f}}{q_2+(1-p_2-q_2)\frac{x}{x_f}+ p_2\,(\frac{x}{xf})^{(p_2/(p_2-q_2))}}\right] \qquad (14)$$

Where σ stress (MPa); σ_f: stress at failure (MPa); $x = \left(\frac{\Delta\rho}{\rho_o}\right) * 100$ = Percentage of change in electrical resistivity due to the stress; $x_f = \left(\frac{\Delta\rho}{\rho_o}\right)_f * 100$ = Percentage of change in electrical resistivity at failure; Δρ: change in electrical resistivity; ρ_o:Initial electrical resistivity (σ = 0 MPa) and p and q: piezoresistive model parameters (Table 3).

0% Foam: The average percentage change in resistance at peak compressive stress of the smart cement after 1 day of curing was 343%. The average percentage change in resistance at peak compressive stress of the smart cement after 28 days of curing was 252%, about 1250 times higher than the compressive strain at failure (0.2%). On an average, the piezoresistivity after 28 days of curing was 12.8%/MPa. The model parameter p_2 after 1 and 28 days of curing were 0.1 and 0.001 respectively. The model parameter q_2 after 1 and 28 days of curing were 0.435 and 0.413 respectively.

5% Foam: The average percentage change in resistance at peak compressive stress of the smart cement after 1 day of curing was 304%, a 11% reduction compared to the smart cement without any foam. The average percentage change in resistance at peak compressive stress of the smart cement after 28 days of curing was 188%, about 940 times higher than the compressive strain at failure (0.2%) for smart cement without any foam. On an average, the piezoresistivity after 28 days of curing was 12.9%/MPa, comparable to the smart cement without any foam. The model parameter p_2 after 1 and 28 days of curing were 0.083 and 0.001 respectively. The model parameter q_2 after 1 and 28 days of curing were 0.274 and 0.586 respectively.

20% Foam: The average percentage change in resistance at peak compressive stress of the smart cement after 1 day of curing was 113%, a 67% reduction compared to the smart cement without any foam. The average percentage change in resistance at peak compressive stress of the smart cement after 28 days of curing was 98%, about 490 times higher than the compressive strain at failure (0.2%) for smart cement without any foam. On an average, the piezoresistivity after 28 days of curing was 18.6%/MPa, higher than the smart cement without any foam. The model parameter p_2 after 1 and 28 days of curing were 0.403 and 0.47 respectively. The model parameter q_2 after 1 and 28 days of curing were 0.605 and 1.07 respectively.

Table.3 Summary of piezoresistive and compressive properties of smart cement with foam

	Compressive Strength (MPa)		Peizoresistivity (Δρ/ρ) (%)		Model Parameters p		q	
Foam Content	1 Day	28 Days	1 Day	28 Days	1 Day	28 Days	1 Day	28 Days
0	10.29	19.65	343	252.4	0.1	0.001	0.435	0.4133
5	4.6	14.6	304	187.9	0.083	0.001	0.274	0.586
20	0.57	5.27	113	98.2	0.403	0.47	0.605	1.07

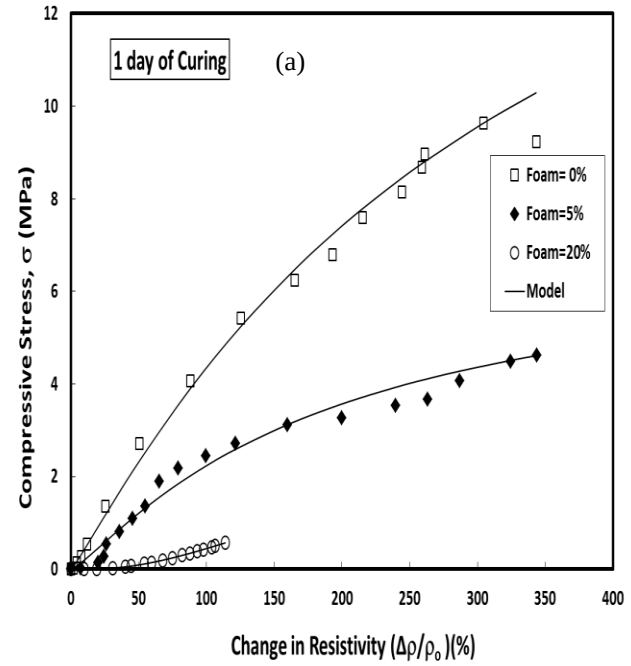

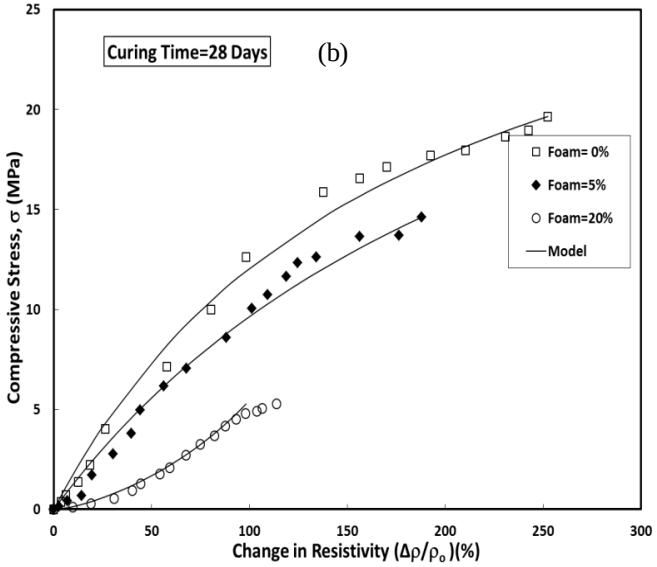

Figure 9- Piezoresistivity Behavior of Class H cement Vs Foam Cement

Conclusions

Based on the experimental and analytical modeling of the rheological and piezoresistivity behavior on smart cement with and without foam, following conclusions are advanced:

1. Smart foam cement slurry was piezoresistive and the resistivity change increased with the foam content. With the addition of 20% foam, the resistivity change at 4 MPa (600 psi) increased from 8% for the smart cement slurry with no foam to 22% with 20% foam, about 175% increase in the piezoresistivity.
2. The rheological test showed that class H oil well cement had shear-thinning behavior and a hyperbolic model was proposed to predict shear stress- shear strain rate relationship. The hyperbolic rheological model predicted the test results very well compared to Herschel-Bulkley model.
3. The yield stress and maximum shear stress limit reduced with the addition of foam. The maximum shear stress limit for smart cement slurry was 195 Pa and it reduced to 107 Pa with the addition of 20% foam, a 45% reduction.
4. The total fluid loss for the smart cement at 0.7 MPa (100 psi) pressure was reduced from 134 mL to 13 mL with the addition of 20% foam, about a 90% reduction.
5. Addition of 20% foam increased the initial electrical resistivity of smart cement from 1.05 Ωm to 2.04 Ωm, a 93% increase. Addition of foam affected the curing of the cement based on the resistivity measurements.
6. The average compressive strength of the smart foam cement after 1 day of curing was 0.57 MPa, about 94% reduction in strength compared smart cement without any foam. The average compressive strength of the smart foam cement after 28 days of curing was 5.27 MPa, a 825% increase in strength. The 28th day compressive strength of smart foam cement was 73% less than compressive strength of the smart cement without any foam.
7. The solidified smart cement with and without foam were piezoresistive. The average percentage change in resistance at peak compressive stress of the smart foam cement with 20% foam after 1 day of curing was 113%, a 67% reduction compared to the smart cement without any foam. The average percentage change in resistance at peak compressive stress of the smart foam cement after 28 days of curing was 98%, about 490 times higher than the compressive strain at failure (0.2%) for smart cement without any foam. On an average, the piezoresistivity after 28 days of curing was 18.6%/MPa, higher than the smart cement without any foam.

Acknowledgments

This study was supported by the Center for Innovative Grouting Materials and Technology (CIGMAT) and Texas Hurricane Center for innovative Technology (THC-IT) at the University of Houston, Houston, Texas.

References

1. Akthar, F. K., and Evans, J. R. (2010), "High Porosity(>90%) Cementitious Foams" *Cement and Concrete Research*, 40(2): 352-358
2. API Recommended Practice 10B (1997), Recommended Practice for Testing Well Cements

Exploration and Production Department, 22nd Edition.
3. API recommended Practice 65 (2002) Cementing Shallow Water Flow Zones in Deepwater Wells.
4. Chung, D.D.L (2001), "Functional Properties of cement-Matrix Composites," Journal fo Material Science, Vol. 36, pp. 1315-1324.
5. Izon, D., Mayes, M. (2007). "Absence of fatalities in blowouts encouraging in MMS study of OCS incidents 1992-2006." Well Control, pp. 86-90.
6. John B., (1992). "Class G and H Basic Oil Well Cements," World Cement.
7. Kyle, M. and Eric, O. (2014). "Improved regulatory oversight using real- time data monitoring technologies in the Wake of Mocondo." SPE 170323, pp. 1-51.
8. Labibzadeh, M., Zhhabizadeh, B. and Khajehdezfuly, A., (2010) "Early Age Compressive Strength Assessment of Oil Well Class G Cement Due to Borehole Pressure and Temperature Changes, Journal of American Science, Vol. 6, No.7, pp.38-47.
9. Li, G. Venkata, D. and Muthyala. A (2008), "Cement Based Syntactic Foam" *Materials Science and Engineering A*, 78(1-2): 77-86
10. Ravi, K. et al. (2007) "Comparative Study of mechanical Properties of Density-reduced Cement Compositions, SPE Drilling & Completion, Vol. 22, No. 2, pp. 119-126.
11. Vipulanandan, C. and Paul, E. (1990), "Performance of Epoxy and Polyester Polymer concrete," ACI Materials Journal, Vol. 87, No. 3, pp. 241–251.
12. Vipulanandan, C., and Garas, V. (2006), "Piezoresistivity of Carbon Fiber Reinforced Cement Mortar", Proceedings, Engineering, Construction and Operations in Challenging Environments, Earth & Space 2006, Proceedings ASCE Aerospace Division, League City, TX, CD-ROM.
13. Vipulanandan, C., and Sett, K. (2004) "Development and Characterization of Piezoresistive Smart Structural Materials", Proceedings, Engineering, Construction and Operations in Challenging Environments, Earth & Space 2004, ASCE Aerospace Division, League City, TX, pp. 656-663.
14. Vipulanandan, C. and Prashanth, P. (2013). "Impedance spectroscopy characterization of a piezoresistive structural polymer composite bulk sensor." Journal of Testing and Evaluation, Vol. 41, pp. 898-904.
15. Vipulanandan, C., Heidari, M., Qu, Q., Farzam, H. and Pappas, J. M. (2014). "Behavior of piezoresistive smart cement contaminated with oil based drilling mud." Offshore Technology Conference, OTC 25200-MS, pp. 1-14.
16. Vipulanandan, C. and Mohammed, A. (2014). "Hyperbolic rheological model with shear stress limit for acrylamide polymer modified bentonite drilling muds." Journal of Petroleum Science and Engineering, Vol. 122, pp. 38–47.
17. Wei, X., Lianzhen, X. and Li, Z. (2008). "Electrical measurement to assess hydration process and the porosity formation." Journal of Wuhan University of Technology-Material Science. Ed., Vol. 23, pp. 761-766.
18. Zhang M., Sisomphon K., Ng T.S, and Sun D.J, (2010). "Effect of superplasticizers on workability retention and initial setting time of cement pastes," Construction and Building Materials 24, 1700–1707.
19. Zhang J., Weissinger E.A, Peethamparan S, and Scherer G.W., (2010). "Early hydration and setting of oil well cement," Cement and Concrete research, Vol. 40, 1023-1033.
20. Zuo, Y., Zi, J. and Wei, X. (2014). "Hydration of cement with retarder characterized via electrical resistivity measurements and computer simulation." Journal of Construction and Building Materials, Vol. 53, pp. 411–418.